

# Recent developments in magnetic shape memory actuation

E. Pagounis<sup>1</sup>, P. Müllner<sup>2</sup>

<sup>1</sup>ETO MAGNETIC GmbH, Stockach, Germany

<sup>2</sup>Dept. of Materials Science and Engineering, Boise State University, Boise, Idaho, USA

Abstract:

Magnetic shape memory (MSM) actuators offer several advantages over conventional and other smart actuator technologies. Considerable progress in optimizing the production process and magneto-mechanical properties of MSM materials has been achieved over the past years, making the material suitable for volume production. Innovative actuator concepts as well as in-depth studies in modeling and control are presented in this review. Efficient design and considerable energy reduction of MSM actuators are key requirements in the commercialization process.

Keywords: magnetic shape memory, properties, actuators, modeling, control, microfluidics

## 1. Introduction

Magnetic shape memory (MSM) provides an alternative way to generate motion and force. In the presence of a relatively weak ( $< 0.6$  T) magnetic field the MSM material elongates and contracts more than 6 % and generates stresses of around 3 MPa. In addition, the inverse effect takes place and the material's magnetic properties change when mechanically deformed. Accordingly, MSM materials are very well suited for actuator, sensor, and energy harvesting applications. Actuators made of these materials have received considerable attention due to their advantages over other smart and conventional actuator technologies. Compared to thermal shape memory materials, MSM offers a much faster response time and better fatigue properties. With regard to piezoelectric materials, MSM produce larger work output, they are less brittle, and do not show degradation associated with humidity or aging effects. Finally, compared to electro-active polymers MSM materials give higher stress output, they have better fatigue resistance and can operate at a wider temperature range.

MSM actuators are also considerably faster than electromagnetic solenoids, they produce larger work output, and have higher fatigue resistance. In addition, they can be designed very energy efficient because they can “keep” a certain position without consuming current, a feature which is not possible e.g. with electromagnetic technologies. Accordingly, several prototype actuators are currently developed for a variety of industrial applications. The aim of the present paper is to provide more insights into the recent advances in MSM materials and actuators.

## 2. Development of MSM materials

Considerable progress has been achieved during the last few years both in increasing the MSM material quality and performance, as well as towards the industrialization of the production process. These

are essential issues when planning a large scale actuator production with optimized performance. Large Ni-Mn-Ga single crystals with diameter above 25 mm and length over 150 mm can now be routinely produced. The homogeneity of the crystals has proven very good along their length. Also crystal growth commercial software has been utilized to improve homogeneity and production speed. Furthermore, significant advancements have been reported towards cutting and electrochemical processes of MSM actuator elements [1], which contribute to their cost-effective production.

The quality of today's Ni-Mn-Ga MSM materials is considerably better than a few years ago. The value of the twinning stress is a good indication of how easy twin boundaries, associated with the large strain of these materials, are moving. Low twinning stress, typically corresponds to materials with large work output and low activation field, resulting in actuator devices with high energy efficiency and reduced size.

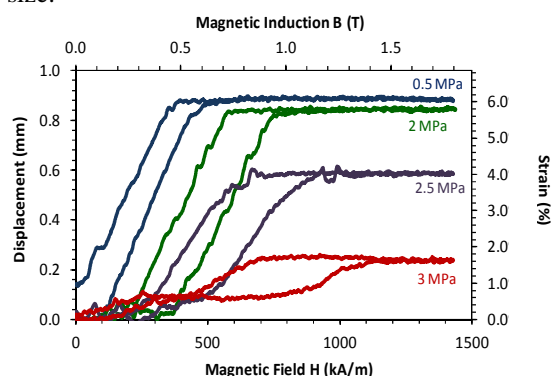
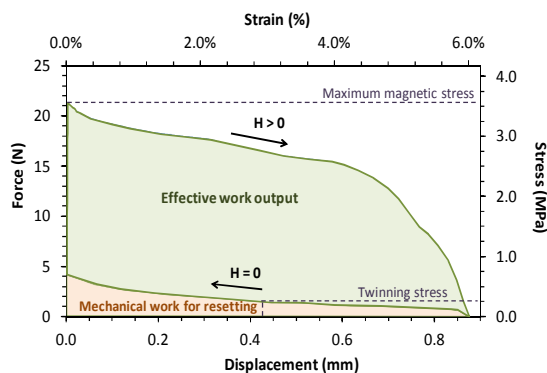


Fig. 1. Strain vs. field measurements in a  $2 \times 3 \times 15$  mm<sup>3</sup> MAGNETOSHAPE® material at pre-stresses of up to 3 MPa.

Materials with a twinning stress value of  $< 0.4$  MPa are well suited for actuator applications and are produced in a large scale today, e.g. by ETO MAGNETIC GmbH. Also materials with even lower

twinning stress have been reported in the literature and are under development [2-4]. Accordingly, there is space for further improvements in actuator performance. Figure 1 shows the strain output of a newly developed MSM material as a function of the applied magnetic field. The material shown in Fig. 1, with a twinning stress of  $< 0.3$  MPa, demonstrates a considerably larger magnetic stress output, since it gives almost 2 % field induced strain at 3 MPa pre-stress.

A further important measurement is the stress-strain curve, which simulates the material's complete actuation cycle. This curve is routinely used to test electromagnetic solenoid actuators and has been successfully applied with MSM materials and actuators. Here the actuator element elongates in the presence of the magnetic field and the magnetic stress and strain output are monitored constantly (e.g. using the sensors of the measurement Zwick set-up). When the material reaches its maximum strain (and the magnetic stress output becomes nearly zero) the field is switched off and the material is mechanically compressed to its initial shape. A typical stress-strain curve of a MAGNETOSHAPE® material is shown in Fig. 2.



**Fig. 2.** Stress vs. strain in a  $2 \times 3 \times 15$  mm<sup>3</sup> Ni-Mn-Ga MSM material, demonstrating large work output. Twinning stress and maximum magnetic stress are shown, too.

This curve provides several properties useful in designing MSM actuators. Besides the magnetic stress and strain output, it gives information about the twinning stress and the work output. The efficiency of the material during the actuation cycle is deduced from the ratio of the effective magnetic field-induced work output, expressed by the area cross-section of the two curves in Fig. 2, to the total work output. In newly developed MSM materials like the one in Fig. 2, efficiency values over 90 % have been measured. The curve can be also used to select the optimum characteristics of the return spring used in the actuator.

The presented magneto-mechanical properties are important and should be measured in MSM materials indented for actuator applications. For a efficient development as well as production scale

testing of MSM actuator elements, a dedicated automatic test bench has been constructed (Fig. 3), where several elements can be tested and analyzed automatically. In addition, magneto-mechanical training of the elements under predefined conditions of stress, field and temperature, can be carried out with the same set-up.



**Fig. 3.** Set-up for automated testing and training of MSM actuator elements (© ETO MAGNETIC).

### 3. Modeling of MSM materials and actuators

Several approaches have been established that are able to simulate the magneto-mechanical behaviour of MSM materials and actuators [5-7]. Reference 7 suggests an approach that can predict the complex behaviour of a complete MSM actuator precisely. For a further commercialization of the MSM technology, effective simulation tools are required to identify optimized actuator designs in relatively short times. Depending on the particular actuator requirement of an application the optimum design can be modelled to achieve e.g. the smallest size or the lowest energy consumption.

Because of the complexity and the nonlinearity of electro-magnetism, together with the large number of design parameters, an evolutionary algorithm has been developed, which has proven to be a robust method for optimization of nonlinear problems with many variables, as well as linear and nonlinear boundary conditions [8, 9].

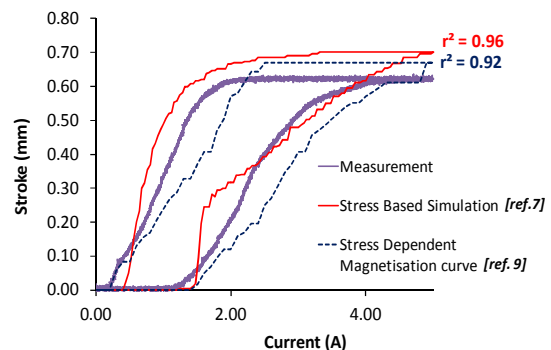


**Fig. 4.** Measured and simulated stroke output of an MSM actuator.

The evolutionary algorithm has been combined with a magnetostatic and thermal FEM tool. Based on

specific target functions that evaluate magnetic, thermal, and geometric design quality under different boundary conditions, it is possible to analyze thousands of actuator variants in a very short time. The actuator volume optimized by the evolutionary algorithm has been compared with the engineered solution. It has been proven that the algorithm delivers in a short time approximately the same design [9].

In Fig. 4 the MSM actuator stroke is simulated, using two models [7, 9]. The accuracy, measured by the coefficient of determination  $r^2$ , to the measurement result is very good.

#### 4. MSM actuator control

Similar to other smart actuator technologies, tracking control of MSM actuators requires the dynamic and the quasi-static phenomena (hysteresis) to be taken into consideration. A schematic of a suggested control unit is presented in Fig. 5. The controller C should be designed to ensure some tracking performance, like when the output  $y(t)$  tracks a desired reference signal  $r(t)$ .

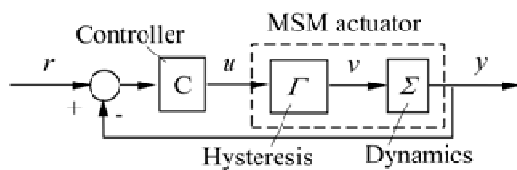


**Fig. 5.** Schematic of an MSM actuator in a control loop (courtesy: L. Riccardi).

Specific MSM actuators, such as the push-push [10] or the field-inverting concept [11], offer the possibility of reducing the electrical power, when used e.g. in positioning applications. This energy-efficient characteristic, realized thanks to the twinning stress of the MSM alloy, shall be considered in the design of a controller. Accordingly, the work on the control of such MSM actuators has the following targets:

- i. Establish design guidelines for the controller C, to provide a defined performance;
- ii. Let the controller C to exploit the energy-efficient property of the actuator [12].

Target (i) is addressed in detail in reference [13], with a particular emphasis on standard proportional-integral-derivative controllers (PIDs). Target (ii) is the main topic of reference [12] and of [14]. In particular, ref. 12 introduces a control strategy that can be added to an existing controller in such a way that further design effort is not necessary. Fig. 6 compares the tracking results of a standard controller C1 and those of the energy-efficient version C1e. The energy efficient version offers a reduction of the Joule losses of up to 60%, achieved using the inherent material's twinning stress.

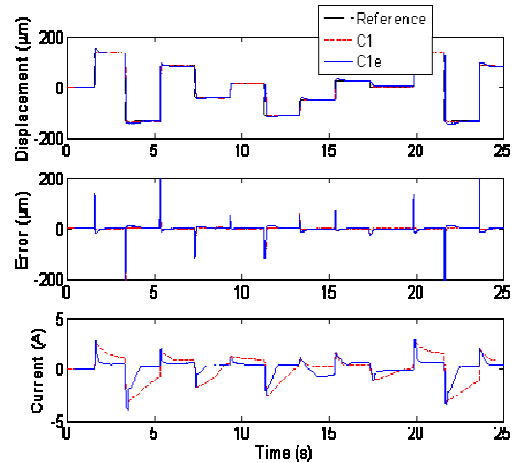


**Fig. 6.** Measurement results of an energy efficient controller (C1e-dashed line) compared to a standard controller (C1-solid line) (courtesy: L. Riccardi).

#### 5. MSM energy harvesting

The principle of energy harvesting using MSM materials is similar to an electromagnetic generator: a changing magnetic flux inside a pick-up coil causes an alternating current to flow in the coil. The changing magnetic flux can be achieved by alternately compressing and elongating the MSM element by an external force [15, 16]. Such small movements have proven to considerably change the magnetic flux [17]. MSM harvesters generated based on this principle can be very small in size. The device is non-resonant and can operate at any frequency. An example of a prototype is shown in Fig. 7, together with the measured output power. At 50 Hz an output power density of  $0.9 \text{ mW/cm}^3$  was measured with the device, while models suggest that also higher values can be achieved [17].

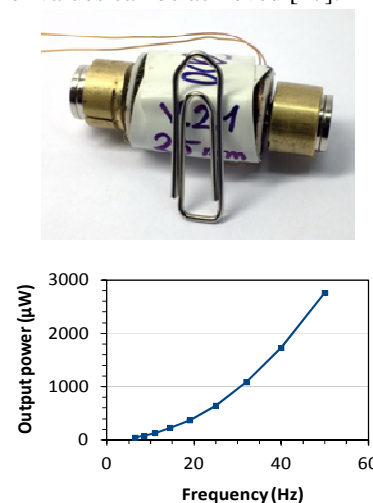


**Fig. 7.** Prototype MSM harvester and output power as a function of vibration frequency (© Adaptamat).

As the device is non-resonant it may be applied both in constantly and non-constantly vibrating

environments. In the later case the force applied on the MSM material shall be large enough. The output voltage of the MSM harvester can be sufficient to directly charge a Li-ion battery or a supercapacitor. Various low-power devices exist to convert the storage device's energy into regulated standard voltages with high efficiency (e.g. LTC3388, www.linear.com). These can operate sensors, microcontrollers and wireless data transmission devices for short periods of time. They can form a completely autonomous wireless sensor network node, which requires no wiring for either power or data, nor periodic replacement of batteries [17].

## 6. Heterogeneous deformation

Much work on magnetic-field-driven actuation of MSM alloys focuses on changing the length of a rod, expressed as magnetic-field-induced strain (MFIS), e.g. [18]. MFIS is a measure for the total length change of an MSM element akin to the definition of engineering strain. This is a global measure that correlates with the local strain only if deformation is homogeneous.

While such an actuator design seems straightforward, it leads to challenges related to the deformation mechanism: twinning. Twinning proceeds through the motion of an interface and is inherently heterogeneous. Heterogeneous deformation causes design problems. For example, a single twin boundary in a two-domain crystal produces a kink. As the twin boundary moves through the crystal, the kink moves, too. If the actuator design requires a longitudinal stroke, the moving kink causes friction, lateral motion, and tilting. Furthermore, the design of the fixture of the element needs to account for the heterogeneous deformation since rigid mounting suppresses actuation at least partially [19].

We show here that in spite of these apparent challenges, heterogeneous deformation provides opportunities for actuator solutions.

### 6.1 Bending

Bending a Ni-Mn-Ga single crystal rod produces a dense twin microstructure with twin wedges in such a way that the shorter crystallographic  $c$  axis orients axially on the concave (i.e. compressed) side of the rod and radially on the convex (i.e. expanded) side of the rod. Straka *et al.* utilized this effect to produce a twin microstructure with fine, wedge-shaped twins [2]. Zheng *et al.* have recently shown that bending can also be achieved through the application of a magnetic field [20]. For a wire with diameter of 250  $\mu\text{m}$ , surface strains of 1.5% result in a radius of curvature of 8 mm. The curvature can be reversed via a change in the magnetic field direction (Fig. 8). Bending amplifies the stroke and produces displacements in the order of the element length. Furthermore, a long element can be rigidly fixed at

one end without restricting the large deflection of the other end, thus, avoiding design constraints.

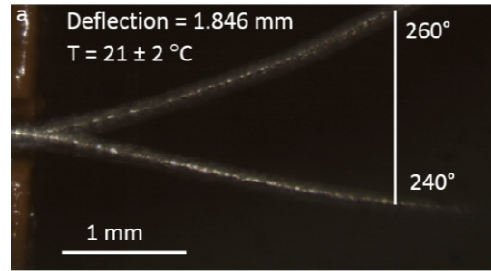


**Fig. 8.** Bending is one example of heterogeneous deformation which can be achieved with magnetic fields. The picture shows two overlapped images of a wire exposed to a magnetic field oriented at 240° and 260° to the horizon. [20]

### 6.2 Local deformation by magnetic field pulses

In a recent study, Smith *et al.* have demonstrated that a rod can exhibit field-driven *shape change* with keeping a constant length and constant fractions of twins [21]. They have fixed the length of a Ni-Mn-Ga rod containing about 15% twin variants with the crystallographic  $c$  perpendicular to the rod axis and the remainder of the volume with  $c$  parallel to the rod axis. Then they applied a local magnetic field pulse perpendicular to the rod axis at a particular location (Fig. 9a). The magnetic field drove all twins into the volume directly exposed to the magnetic field. The collected twins produced a shape change in the form of a “neck”. The magnet was then displaced (Fig. 9b) and a magnetic field pulse was applied at the new location (Fig. 9c). This second field pulse drove the twins into the volume near the new position of the magnet. In this manner, they drove a narrow neck along the rod. This mechanism mimics the swallowing mechanism of mammals.

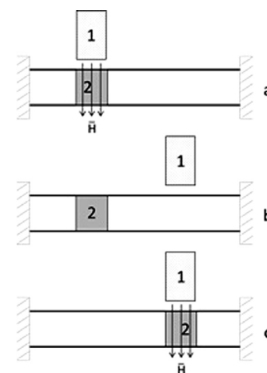


**Fig. 9.** Local actuation of a rod with fixed length. a) The electromagnet (1) collects the twins with  $c$  perpendicular to the rod axis at the position (2). (b) The magnet was then displaced to a new position. (c) When a magnetic field pulse was applied at the new position, the twins now collected at this site.

### 6.3 Shape change driven by a rotating magnet

Ullakko *et al.* demonstrated that a single permanent magnet stabilizes a well-defined twin microstructure in a MSM element [22]. Fig. 10 shows the magnetic field distribution in a Ni-Mn-Ga element generated by a diametrically magnetized permanent magnet rod where the magnetization of the magnet is perpendicular to the MSM element. In a very large portion of the element, the magnet stabilizes a twin domain with  $c$  parallel to the long axis of the element. In a small volume nearest to the permanent magnet, the magnetic field stabilizes a twin domain with  $c$  perpendicular to the axis of the MSM element.

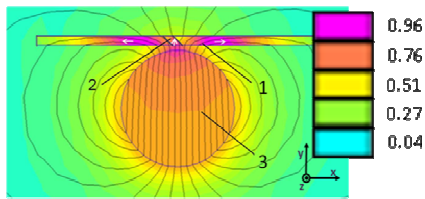


**Fig. 10.** Magnetic field distribution in a Ni-Mn-Ga element (horizontal bar, 1) evoked by a diametrically magnetized rod (3). The heterogeneous field stabilizes a small twin variant (2) with  $c$  perpendicular to the rod axes while  $c$  is parallel to the rod axes outside of the area (2). [22]

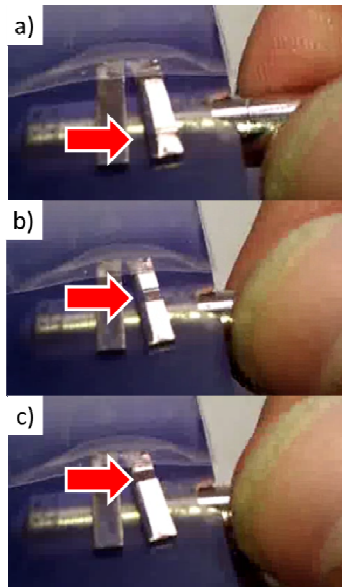


**Fig. 11.** Three frames of a video recording of a twin variant moving in the changing field of a slowly rotating diametrically magnetized magnet (video courtesy of K. Ullakko).

Upon rotation of the diametrically magnetized rod, the small intermediate twin variant with  $c$  perpendicular to the element axis moved along the MSM element (Fig. 11).

### 6.4 Micropump

Ullakko *et al.* [22] applied this concept (section 6.3)

to devise a micropump. They attached an MSM element to a glass plate containing two holes (Fig. 12). They fixed the length of the MSM element with epoxy and sealed element and glass with silicone. A diametrically magnetized magnet collected twins with  $c$  perpendicular to the glass plate at a specific location. The element formed a neck at this location which generated a cavity between element and glass plate. Upon rotation of the magnet, the cavity moved along the element and transported liquid.

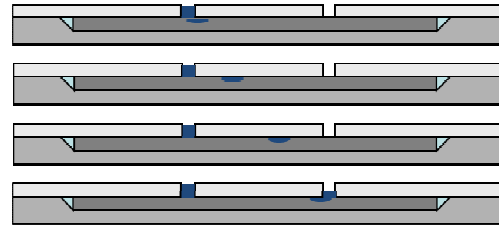


**Fig. 12.** Schematic of the micropump and pumping mechanism. The MSM element (dark gray) is attached to a glass plate (light gray) and fixed in length. The element contains a neck which causes a cavity. When actuated magnetically, the cavity moves along the glass plate, and transports liquid from one reservoir to another.

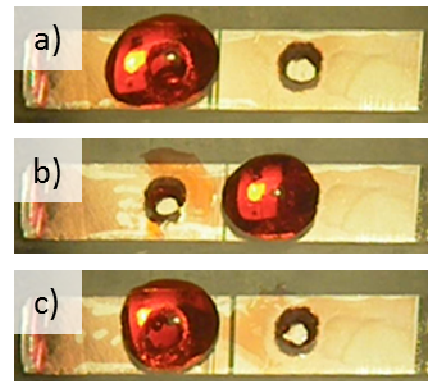


**Fig. 13.** Micropump imaged from top. The MSM element is visible through the glass plate, which contains two holes with about 1 mm diameter. The width of the MSM element is 2.5 mm.

Fig. 13 shows three frames of a video demonstrating pumping of water. The pump contains no valve and works in both directions. A droplet of stained water was deposited on the glass plate over the left hole (Fig. 13a). The pump was then actuated with a diametrically magnetized rod (similarly to the experiment shown in Fig. 11). The rotating magnet caused the cavity to move from the left to the right. When the cavity reached a position under the right hole, the cavity disappeared and reformed under the left hole. Moving along the glass plate, the cavity transported the water from the left hole to the right hole and deposited the water there (Fig. 13b). Changing the sense of rotation of the diametrically magnetized rod reversed the pump direction (Fig. 13c).

## 6.5 Discussion on heterogeneous deformation

We presented a few examples for actuation via heterogeneous deformation of MSM elements. At first glance, heterogeneous deformation may seem complicated and difficult to achieve. However, deformation of magnetic shape memory alloys by nature is inherently heterogeneous. Furthermore, it is much easier to create a heterogeneous magnetic field than to create a homogeneous field, particularly if operating with limited power.

When a permanent magnet is oriented perpendicularly to an MSM element (Fig. 10), the magnetic dipole field stabilizes a well-defined twin microstructure. In this case, a small twin with  $c$  parallel to the magnet dipole axis is sandwiched between two extended domains with  $c$  perpendicular to the dipole axis. The position of the intermediate twin is determined by the position of the magnet. It would be extremely difficult, to reproducibly create this microstructure with a homogeneous magnetic field or with other methods, for example the application of local forces.

The position of the intermediate twin can be changed by displacing the magnet (Fig. 9) or by rotating the magnet (Fig. 11). Again, it is difficult to imagine a procedure relying on a homogeneous magnetic field or on mechanical loads that would produce the same result.

For an actuator relying on homogeneous deformation of the MSM element, the fixture of the MSM element causes a problem. On the one hand, the fixture may suppress deformation to the extent that the fixture obstructs the operation of the actuator. On the other hand, if deformation is not suppressed, repeated deformation may cause fatigue damage and failure of the fixture or of the MSM element at the location of the fixture.

Deforming an MSM element heterogeneously provides a solution. The element can remain undeformed at the location of the fixture without impacting the active region. For example, the wire in Fig. 8 was rigidly glued to the sample holder (on the left outside the field of view in Fig. 8). Bending occurred only outside of the glued area. The fixture did not hinder bending. The MSM element of the pump (Fig. 13) was rigidly fixed at its ends only while it was sealed with elastic silicone and elastomer everywhere else. Here again, the fixture did not obstruct the operation.

The heterogeneous nature of twinning allows the controlled, heterogeneous (e.g. localized) magnetic-field-induced deformation of magnetic shape memory alloys. Localized deformation can be achieved via applying a variable, heterogeneous magnetic field (e.g. via the rotation of a permanent magnet). Localized magnetic-field-driven deformation provides actuator solutions not attainable with homogeneous deformation.

## Acknowledgment

The authors would like to thank Dr. L. Riccardi (University of Saarland) and Dr. A. Niskanen (Adaptamat Ltd.) for providing relevant Figures. P.M. acknowledges financial support from the Micron Foundation.

## References

- [1] A. Böhm et al., in this conference.
- [2] L. Straka, H. Hänninen, A. Soroka, A. Sozinov, *J. Phys.: Conf. Ser.* 303 (2011), 012079.
- [3] R. Chulist, E. Pagounis, A. Böhm, C.G. Oertel, W. Skrotzki, *Scripta Mater.* 67 (2012), 364.
- [4] D. Kellis, A. Smith, K. Ullakko, P. Müllner, *J. Crystal Growth* 359 (2012), 64.
- [5] T. Schiepp, M. Maier, E. Pagounis, M. Laufenberg, *Actuator 2012*, Bremen, 660.
- [6] I. Suorsa, J. Tellinen, I. Aaltio, E. Pagounis, K. Ullakko, *Actuator 2004*, Bremen, 573.
- [7] T. Schiepp, M. Maier, E. Pagounis, A. Schlüter, M. Laufenberg, *IEEE Trans. Magn.* 50, 2014, 7024504.
- [8] I. Rechenberg. *Evolutionsstrategie '94*, Frommann-Holzboog Verlag, 1994.
- [9] T. Schiepp, A. Schlüter, S. Schäfer, M. Maier, M. Laufenberg, *CEFC 2014*, Annecy, France.
- [10] J. Gauthier, A. Hubert, J. Abadie, C. Lexcelent, N. Chaillet, *Actuator 2006*, 787.
- [11] B. Holz, L. Riccardi, H. Janocha, D. Naso, *Adv. Eng. Mater.* 14 (2012), 668.
- [12] L. Riccardi et al., in this conference.
- [13] L. Riccardi, D. Naso, B. Turchiano, H. Janocha, *IEEE Trans. Control Syst. Technol.*, in press (DOI: 10.1109/TCST.2013.2282661).
- [14] L. Riccardi, B. Holz, H. Janocha, in *International Conference Innovative Small Drives and Micro-motor systems 2013*, Nuremberg, Germany, 63.
- [15] P. Müllner, V. A. Chernenko, G. Kostorz, *Scripta Mater.* 49 (2003), 129.
- [16] D. Carpenter et al. *Proc. ICOMAT'08*, TMS (2009) 365.
- [17] A. Niskanen, *WoWSS 2012*, 2nd Workshop on Wireless Sensor Systems, Espoo, Finland, 2012.
- [18] K. Schlüter, B. Holz, A. Raatz, *Adv. Eng. Mater.* 14 (2012), 682.
- [19] M. Chmielus, P. Müllner, *Mater. Sci. Forum* 684 (2011), 175.
- [20] P. Zheng, N. Kucza, C. L. Patrick, P. Müllner, D. C. Dunand, submitted to *Acta Mater.* (2014).
- [21] A. Smith, J. Tellinen, P. Müllner, K. Ullakko, *Scripta Mater.* 77 (2014) 68.
- [22] K. Ullakko, L. Wendell, A. Smith, P. Müllner, G. Hampikian, *Smart. Mater. Struct.* 21 (2012), 115020.